Simultaneous Optimization and Heat Integration Framework Based on Rigorous Process Simulations

Yang Chen [a,b,*], John C. Eslick [a,b], Ignacio E. Grossmann [a], David C. Miller [b]

[a] *Department of Chemical Engineering, Carnegie Mellon University, 5000 Forbes Avenue, Pittsburgh, PA 15217, United States*

[b] *National Energy Technology Laboratory, 626 Cochrans Mill Road, Pittsburgh, PA 15236, United States*

Abstract

This paper introduces a novel simultaneous optimization and heat integration approach, which can be used directly with the rigorous models in process simulators. In this approach, the overall process is optimized utilizing external derivative-free optimizers, which interact directly with the process simulation. The heat integration subproblem is formulated as an LP model and solved simultaneously during optimization of the flowsheet to update the minimum utility and heat exchanger area targets. A piecewise linear approximation for the composite curve is applied to obtain more accurate heat integration results. This paper describes the application of this simultaneous approach for three cases: a recycle process, a separation process and a power plant with carbon capture. The case study results indicate that this simultaneous approach is relatively easy to implement and achieves higher profit and lower operational cost and, in the case of the power plant example, higher net efficiency than the sequential approach.

Key Words

heat integration, simulation based optimization, simultaneous approach, piecewise linear approximation, carbon capture

* Corresponding author. Tel.: +1 412-386-4798.
Email address: yangchen@andrew.cmu.edu.

Highlights

- A simultaneous process optimization and heat integration framework is proposed.
- This framework is based on rigorous models in process simulators.
- Minimum utility and heat exchanger area are predicted by a targeting approach.
- A piecewise linear approximation for the composite curve is implemented.
- Higher profit, conversion, power efficiency, lower operating cost are achieved.

1. Introduction

Heat integration plays a key role in improving energy efficiency and reducing operational costs in the energy and chemical industries. A number of methodologies have been developed in process systems engineering research for heat exchanger network synthesis (HENS). Linnhoff and Hindmarsh (1983) proposed the pinch design method, which is based on physical insight for the maximum heat recovery in heat exchanger networks. Papoulias and Grossmann (1983) and Cerda and Westerberg (1983) developed mathematical programming based methods for HENS. Detailed reviews for developments of HENS methods can be found in Gundersen and Naess (1988), Grossmann et al. (1999), Furman and Sahinidis (2002), Morar and Agachi (2010) and Klemeš and Kravanja (2013).

Two different approaches for combining heat integration and process optimization have been developed: sequential and simultaneous. Traditionally, a sequential strategy is applied when performing process optimization without heat integration, that is, the process is optimized in the first stage assuming all heating and cooling loads are provided by utilities; in the second stage, heat integration is performed after the optimal stream conditions (flow rates, temperatures, etc.) are identified (Biegler et al., 1997). Since heat integration is ignored during process optimization, the sequential approach may not fully optimize the whole process and may overestimate the utility cost. To overcome this drawback, Duran and

Grossmann (1986) proposed a simultaneous strategy in which heat integration is performed in conjunction with process flowsheet optimization. In this strategy, a set of heat integration constraints that predict the minimum utility targets are added to the process optimization model. These constraints are based on a pinch location method so that heat integration can be performed under variable stream flowrates and temperatures. The authors also extended the pinch location method to cases with multiple utilities. A smooth approximation method was proposed to overcome non-differentiablilties in the optimization problem so that the entire problem can be solved as a regular NLP problem. The simultaneous strategy has been demonstrated to achieve better economic performance, including both higher conversions of raw materials and lower total costs in recycle processes, compared to the sequential strategy (Duran and Grossmann, 1986; Lang et al., 1988; Biegler et al., 1997). Grossmann et al. (1998) proposed an MINLP model for simultaneous process optimization and heat integration in which logic disjunctions were used to explicitly model the placement of streams for various potential pinch locations. This article also extended the application of the simultaneous strategy to cases with isothermal streams. Kamath et al. (2012) further extended the simultaneous strategy to cases with multistream heat exchangers (MHEX) and with process streams undergoing phase change; streams with phase change were split into substreams corresponding to each of phases, and a disjunctive representation was proposed to identify the phase for each substream. Papalexandri and Pistikopoulos (1998) developed a decomposition method for the solution of simultaneous process optimization and heat integration, where the heat integration problem was solved in an inner loop for a fixed process flowsheet and the process flowsheet was then optimized in an outer loop using the information from heat integration. Lang et al. (1988) implemented the simultaneous approach within the process simulator FLOWTRAN by adding the heat integration constraints developed by Duran and Grossmann (1986) to the process model in the simulator. The optimization was implemented using an SQP method, which assumes differentiability in the functions. Thus, newer derivative-free optimization solvers have not been used. In addition, this approach cannot handle cases where models of different units or subsystems are implemented in different process simulators.

The simultaneous optimization and heat integration approach has been applied to the optimal design of a wide range of processes, such as distillation systems (Novak et al., 1996), reaction/separation systems (Papalexandri and Pistikopoulos, 1998), hybrid thermochemical processes converting coal, biomass and natural gas to transportation fuel (CBGTL) (Baliban et al., 2011; 2012), biodiesel production processes (Martín and Grossmann, 2012), water networks (Yang and Grossmann, 2012; Kim et al., 2009), biorefinery processes (Ng et al., 2012; Wang et al., 2013; Gebreslassie et al., 2013), ethanol and food coproduction processes (Čuček et al., 2011), energy polygeneration processes (Chen et al., 2011a; 2011b), and offshore natural gas liquefaction processes (Wechsung et al., 2011). The simultaneous approach has also been used for the retrofit of chemical processes (Ponce-Ortega et al., 2008a).

However, the current simultaneous approach relies on optimization models developed in equation-based modeling environments such as GAMS. Until recently, this capability has not been compatible with the more rigorous models implemented within the commercial flowsheet simulators that are widely used in power, chemical and oil industries, such as Aspen Plus, Aspen HYSYS, Aspen Custom Modeler (ACM), gPROMS and Thermoflex. Many simulation-based optimization technologies have been developed in recent years and applied to optimization of various processes utilizing rigorous simulator-based models (Gosavi, 2003; Rajasree and Moharir, 2000; Wan et al., 2005; Mele et al., 2006; Deng, 2007; Eslick and Miller, 2011). These advances in simulation-based optimization provide the foundation for the simultaneous optimization and heat integration framework proposed in this article.

This paper introduces a novel simultaneous optimization and heat integration approach, which can be used directly with the rigorous models in process simulators. Since the process models in simulators are usually large black box models that do not readily provide derivative information, this approach utilizes a derivative-free optimizer (DFO) (Conn et al., 2009; Kolda et al., 2003; Rios and Sahinidis, 2013) to optimize the overall process system. Links are established among the process simulators, the heat

integration module and the DFO to realize efficient data transfer. For each iteration of the DFO, the process simulators converge the model for a set of design and operating conditions determined by the DFO. Stream temperatures and heating and cooling loads are exported to the heat integration submodel which is solved as a linear programming problem in GAMS for the minimum utility target and minimum heat exchanger area target. The results from both the process simulation and the heat integration submodel are then returned to the DFO and used to evaluate the overall objective function. Compared with the equation-based simultaneous approach, the proposed simulation-based simultaneous approach has several advantages. First, it treats simulations as black boxes and is easy to implement. Second, it does not require simplification of process models. Hence, high-fidelity models can be directly used. Finally, it can be applied to processes in which unit models are developed in different process simulators. This paper describes the overall framework and demonstrates its capabilities in three industrial-scale cases: a methanol production process (with a recycle stream), a separation process for benzene products and a supercritical pulverized coal power plant with post-combustion carbon capture and compression.

The remaining part of this paper is organized as follows. Section 2 introduces the overall simulation-based optimization framework with heat integration. Section 3 describes the heat integration module used in the simultaneous approach, including the LP models for the minimum utility target and the minimum heat exchanger area target. The piecewise linear approximation for the composite curve of streams is also described in Section 3. Finally, Section 4 discusses optimization and heat integration results for the three industrial-scale cases. The paper is concluded in Section 5.

2. Simultaneous Optimization and Heat Integration Framework

2.1. Overall Framework

The simulation-based simultaneous optimization and heat integration framework is illustrated in Figure 1 (Chen et al., 2014), where process simulators, the heat integration module and DFOs are tightly linked to

each other. The DFO currently used in this framework is the Covariance Matrix Adaptation Evolutionary Strategy (CMA-ES) (Hansen, 2006), which is a global search optimization method suitable for difficult nonlinear nonconvex problems in continuous domains. Two process simulators, Aspen Plus and ACM (AspenTech, 2014), can be utilized for simulation. Excel and Python are tightly integrated into the framework and are employed to perform cost evaluation and other post-simulation analysis. Support for additional process simulators, such as gPROMS Model Builder (PSE, 2014), is an active area of development. The heat integration module is developed in GAMS (McCarl et al., 2013), and it predicts the minimum utility target and minimum heat exchanger area target when provided with stream and equipment conditions.

The DFO is used to determine the values of the decision variables that maximize or minimize the value of an overall objective function. Within each iteration of the optimization algorithm the process simulation is converged and heat integration problem is solved. First, the DFO selects an initial set of decision variables that are passed to the process simulators. The simulators converge the flowsheet using the values from the DFO. Relevant stream information (hot and cold stream flow rates, temperatures and enthalpies) and equipment information (heating or cooling loads and temperatures of equipment) are transferred from the simulators to the heat integration module. This module, which solves a linear programming problem, is then called to calculate the minimum utility cost (or consumption) and the minimum heat exchanger area while satisfying all heating and cooling loads. Using information from both the process simulations and the heat integration, the system performance is evaluated in Python or Excel, to determine the value of the objective function and system constraints. Finally, the DFO determines new values for the decision variables. This procedure continues until the optimal solution is found or the maximum number of iterations is reached. Note that this framework is generally not well suited to optimization problems with a large number of decision variables, especially integer variables (e.g., superstructure optimization). Therefore, this framework is best used to obtain accurate optimal design

results after the best process topology has been determined, by either superstructure optimization or engineering experience.

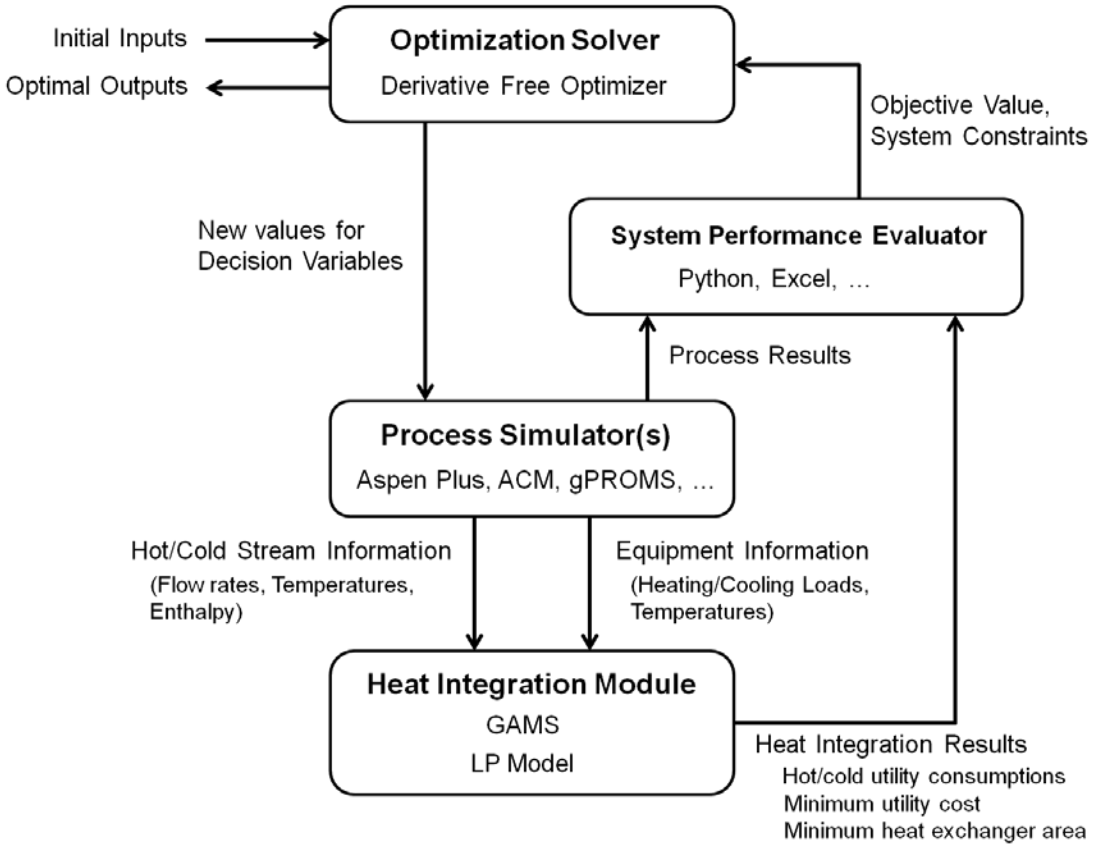

Figure 1. Framework for simulation-based simultaneous optimization and heat integration.

2.2. Implementation

The simultaneous process optimization and heat integration framework is implemented within the Framework for Optimization and Quantification of Uncertainty and Sensitivity (FOQUS) (Miller et al., 2014), which is developed in Python. The input, output and execution of DFOs, process simulations and the heat integration module are managed by the graphical user interface (GUI) of FOQUS. In FOQUS, all models and simulations are linked in a meta-flowsheet, in which a node represents a simulation model and is linked to the actual model file (in some process simulator). Material, energy and information can be

transferred from node to node. The heat integration module is implemented as a special node in FOQUS, which is linked to the heat integration GAMS file. Recycle streams are allowed among nodes in the meta-flowsheet. Two other components play important roles in implementation of FOQUS and the simultaneous framework: SimSinter and Turbine (Boverhof et al., 2013). SimSinter establishes the actual linkage between the nodes in FOQUS and various process simulators. SimSinter, which provides a standard .NET interface, uses a JSON-based configuration file to specify the simulation to be run and to define the input and output variables. Turbine allows users to run hundreds of simulations in parallel. It manages the simulation files, runs jobs, and stores results. FOQUS, SimSinter and Turbine are developed under the U.S. Department of Energy's Carbon Capture Simulation Initiative (CCSI).

3. Heat Integration Module

3.1. Minimum Utility Cost

The heat integration module first predicts the minimum utility cost (or consumption) from the process simulation results. Since the heat integration module only deals with fixed temperatures and heat capacity flowrates, the LP transshipment model for a given heat recovery approach temperature (HRAT) developed by Papoulias and Grossmann (1983), as shown in Eq.(1), is utilized to formulate the minimum utility problem.

$$\min \sum_{m\in S} c_m Q_m^S + \sum_{n\in W} c_n Q_n^W \tag{1}$$

$$\text{s.t. } R_{ik} - R_{i,k-1} + \sum_{j\in C_k} Q_{ijk} + \sum_{n\in W_k} Q_{ink} = Q_{ik}^H \qquad \forall i \in H_k' \qquad \forall k \in \{1,...,K\}$$

$$R_{mk} - R_{m,k-1} + \sum_{j\in C_k} Q_{mjk} - Q_m^S = 0 \qquad \forall m \in S_k' \qquad \forall k \in \{1,...,K\}$$

$$\sum_{i\in H_k} Q_{ijk} + \sum_{m\in S_k} Q_{mjk} = Q_{jk}^C \qquad \forall j \in C_k \qquad \forall k \in \{1,...,K\}$$

$$\sum_{i\in H_k} Q_{ink} - Q_n^W = 0 \qquad \forall n \in W_k \qquad \forall k \in \{1,...,K\}$$

$$R_{ik},\ R_{mk},\ Q_{ijk},\ Q_{mjk},\ Q_{ink},\ Q_m^S,\ Q_n^W \geq 0$$

$$R_{i0} = R_{iK} = 0$$

where *K* is the number of temperature intervals; c_m and c_n are the unit cost of hot utility *m* and cold utility *n*, which are parameters given by users; Q_{ik}^H and Q_{jk}^C are the heat content of hot process stream *i* and cold process stream *j* at temperature interval *k*, which are parameters transferred from simulation results; Q_m^S and Q_n^W are the heat load of hot utility *m* and cold utility *n*; Q_{ijk}, Q_{mjk}, and Q_{ink} are the amount of heat exchanged between hot process stream *i* and cold process stream *j*, hot utility *m* and cold process stream *j*, and hot process stream *i* and cold utility *n* at interval *k*; R_{ik} and R_{mk} are the heat residual of hot process stream *i* and hot utility *m* exiting interval *k*. The index sets are defined below:

$H_k = \{ i \mid \text{hot stream } i \text{ supplies heat to interval } k \}$

$H'_k = \{ i \mid \text{hot stream } i \text{ is present at interval } k \text{ or at a higher interval} \}$

$C_k = \{ j \mid \text{cold stream } j \text{ demands heat from interval } k \}$

$S_k = \{ m \mid \text{hot utility } m \text{ supplies heat to interval } k \}$

$S'_k = \{ m \mid \text{hot utility } m \text{ is present at interval } k \text{ or at a higher interval} \}$

$W_k = \{ n \mid \text{cold utility } n \text{ extracts heat from interval } k \}$

Eq.(1) minimizes the total utility cost (or load) while satisfying heat balances for the hot and cold streams in all temperature intervals. The minimum utility cost will then be returned to the system performance evaluator to calculate the overall objective function (minimum cost or maximum profit). It should be noted that process equipment that releases or absorbs heat is treated as a process stream. In this heat integration module, process streams are considered either as nonisothermal heat sources or sinks or as isothermal heat sources or sinks. However, the difference between inlet and outlet temperatures of isothermal heat sources/sinks is defined to be 1 K to accommodate the formulation in Eq.(1). We initially

calculate the heat load of the streams directly from the total change of enthalpy from the simulation results, which implies constant heat capacity for the streams. However, this assumption may not be true for streams with phase changes or highly non-ideal thermodynamics, as will be discussed later. It is also noted that this embedded LP problem causes discontinuities in the overall optimization problem, which motivates the use of DFO methods, since derivative-based methods (e.g., SQP) may fail to converge.

3.2. Minimum Heat Exchanger Area

The second part of the heat integration module is to predict the minimum heat exchanger area target based on the results of the previous minimum utility cost model. The LP area target model proposed by Jezowski et al. (2003), which is modified from the LP transportation model, is utilized due to its simplicity and high accuracy. The minimum heat exchanger area model is shown in Eq.(2) as below:

$$\min \frac{1}{\mathrm{Ft}} \sum_{k=1}^{K} \sum_{l=1}^{K} \frac{1}{\mathrm{LMTD}_{k,l}} \sum_{i \in H_k} \sum_{j \in C_l} \frac{q_{ik,jl}}{h_i + h_j} \tag{2}$$

$$\text{s.t.} \sum_{l=k}^{K} \sum_{j \in C_l} q_{ik,jl} = Q_{ik}^{H} \qquad \forall i \in H_k \qquad \forall k \in \{1,...,K\}$$

$$\sum_{k=1}^{l} \sum_{i \in H_k} q_{ik,jl} = Q_{jl}^{C} \qquad \forall j \in C_l \qquad \forall l \in \{1,...,K\}$$

where K is the number of temperature intervals. Q_{ik}^{H} is the heat content of hot stream i at temperature interval k, Q_{jl}^{C} is the heat content of cold stream j at temperature interval l. It is noted that hot utilities or cold utilities are treated as hot streams or cold streams in Eq.(2). For hot and cold process streams, the values of Q_{ik}^{H} and Q_{jl}^{C} are the same as those in Eq.(1), which are transferred from process simulation results. For hot and cold utilities, the values of Q_{ik}^{H} and Q_{jl}^{C} are equal to Q_m^S and Q_n^W predicted in Eq.(1) if the hot utility and cold utility are present in interval k and l; otherwise they are equal to zero. $q_{ik,jl}$ is the amount of heat exchanged between hot stream i at interval k and cold stream j at interval l. Ft is the

correction factor for a non-countercurrent flow pattern. h_i and h_j are stream film heat transfer coefficients for hot stream *i* and cold stream *j*. $\mathrm{LMTD}_{k,l}$ is the logarithmic-mean temperature difference between interval *k* and *l*. H_k and C_l are index sets for hot stream *i* and cold stream *j* present at interval *k* and *l*.

To ensure an accurate heat exchanger area target, the sizes of temperature intervals in Eq.(2) should be smaller than those in Eq.(1). This causes a large number of temperature intervals and decision variables in the model. The number of temperature intervals is a critical issue for Eq.(2), that is, a larger number of intervals will increase accuracy of the solution but also increase the CPU time. To keep both high accuracy and short solution time, the number of temperature intervals is determined by using the method proposed by Jezowski et al. (2003). First, the mean size of temperature intervals is calculated as: $dT_{\mathrm{mean}} = \max\left(3\,dT_{\mathrm{min}}, \mathrm{EMAT}\right)$, where dT_{min} is the smallest size of temperature intervals; EMAT is the exchanger minimum approach temperature, which is given by users. Then, all intervals with the size dT larger than dT_{mean} are further divided to N_d intervals, where $N_d = \mathrm{ceil}\left(dT / dT_{\mathrm{mean}}\right)$. This idea is similar to the double-temperature approach (Gundersen and Grossmann, 1990), where HRAT is used to determine the minimum utility cost in Eq.(1) while EMAT (which is smaller than or equal to HRAT) is used to determine the minimum heat exchanger area in Eq.(2).

The result of Eq.(2) may not be directly used to calculate the objective function, but it can be helpful to estimate the capital cost of the heat exchanger network, which can be a large part of the capital cost of the process. It is noted that the minimum number of stream matches and the minimum capital cost of the heat exchanger network are not calculated in this paper because the utility cost dominates the total cost of heat exchanger network and the heat exchanger area can provide a sufficiently accurate estimation for the capital cost.

3.3. Piecewise Linear Approximation for the Composite Curve

We assume constant heat capacity flowrates (FCps) hold between supply and target temperatures for all process streams in Eq.(1) and (2). This assumption tends to hold for process streams with only one phase and with small to medium temperature changes. However, FCps of real process streams may vary significantly with temperature, especially for streams with phase change or highly non-ideal thermodynamic behaviour. Figure 2 shows the T-Q diagram of a mixture stream of carbon dioxide (CO_2) and water (H_2O), which is a common stream in carbon capture and compression processes. This stream shows a highly nonlinear composite curve with variable FCps since a phase change occurs and part of the water condenses below the dew point (around 90°C). The linear approximation of the composite curve with constant FCp, as shown in Figure 2 (a), will exhibit large deviations from the real composite curve. Assuming this stream is a hot process stream, the possible pinch location at the dew point will be omitted and the calculated temperature difference between hot and cold streams will be incorrect. This will overestimate the real heat recovery and even give rise to an infeasible heat exchanger network design. Approximate methods for handling streams with phase change have been studied in previous papers (Ponce-Ortega et al., 2008b; Kamath et al., 2012). In these studies, the whole temperature range of streams with phase change is divided into three sub-regions: superheated, two-phase, and subcooled regions. Constant FCps are still assumed for each region. This approach is considered as a piecewise linear approximation of the composite curve that is able to achieve reasonable heat integration results. However, temperatures of the dew point and bubble point need to be identified. In addition, three sub-regions are not sufficient to obtain accurate results for streams with highly nonlinear thermodynamics.

In order to overcome these drawbacks, a piecewise linear approximation approach is proposed in this article. In this approach, the entire temperature range of process streams is divided into a number of small temperature regions with identical size. We still assume constant FCps hold in each temperature region. When the number of temperature regions is sufficiently large, the piecewise linear approximation will be

very close to the real composite curve, enabling accurate heat integration results to be obtained. However, too many temperature regions may also cause unreasonably long solution times. Hence we need to carefully choose the appropriate number of regions. Based on a number of computational experiments, we have found 5-10 regions are sufficient for most applications. Figure 2 (b) shows the piecewise linear approximation of the composite curve with five temperature regions, which is demonstrated to be a good approximation to the original composite curve. To implement this approximation scheme, we use a series of heaters/coolers with identical temperature change for each cold/hot stream in the process model so that each heater/cooler returns the temperature and enthalpy results for the corresponding intermediate region, and the sum of enthalpy changes within all intermediate temperature regions matches the total change of enthalpy predicted by simulation results.

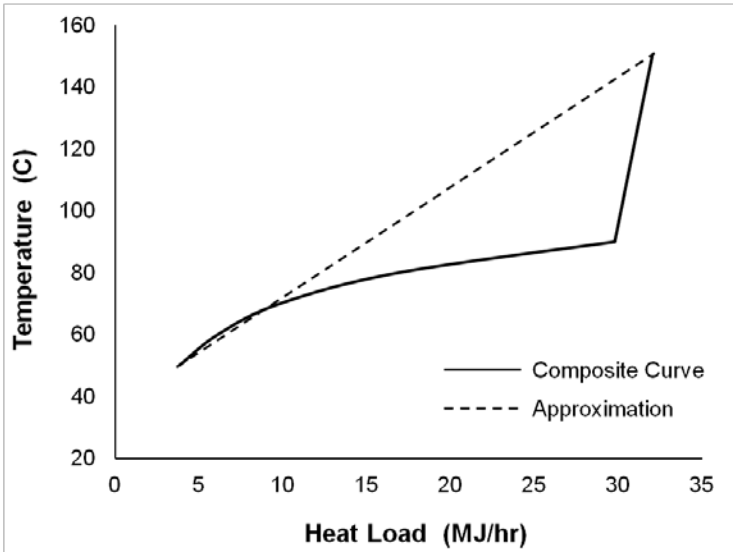

(a) Linear approximation (Constant heat capacity flowrate)

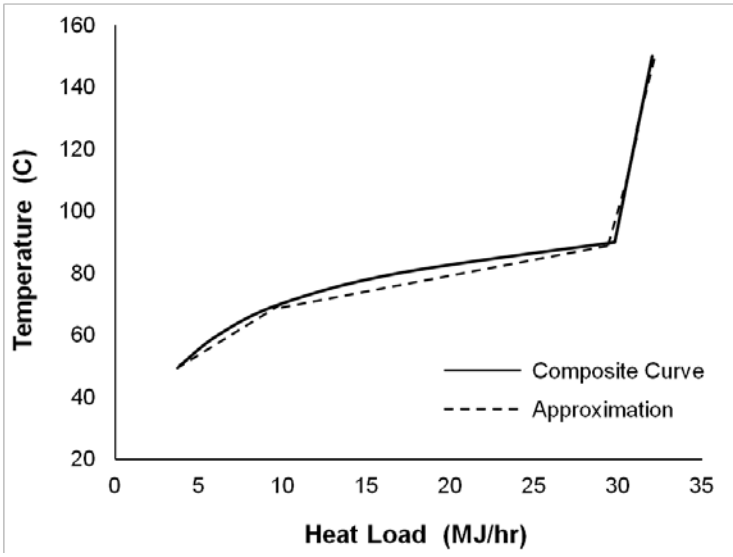

(b) Piecewise linear approximation (5 temperature regions)

Figure 2. Representation of different approximation methods for streams with variable heat capacity flowrates on T-Q diagram

4. Case Study

4.1. Case 1: Methanol Production Process (Recycle Process)

4.1.1. Process Overview

Figure 3 shows the flowsheet of a methanol production process (Türkay and Grossmann, 1996; Yang and Grossmann, 2012). In this process 95% pure methanol (CH_3OH) is produced from the synthetic gas (syngas) feed stream, which contains hydrogen (H_2), carbon monoxide (CO) and methane (CH_4). The information of the syngas stream is shown in Table 1. The syngas feed stream passes through a two-stage compressor with an intermediate cooler. Then the feed stream is mixed with the recycle stream and preheated before entering the methanol synthesis reactor. The product stream of the reactor passes through a valve to reduce the pressure and then cooled before entering the flash unit. After flash, the liquid stream is obtained as the methanol product; part of the gas stream is purged and sold as the by-product, and the remainder is recycled via a compressor. The specifications for the product and by-product streams are listed in Table 2. The methanol production process is modeled in Aspen Plus. In order

to be both simple and realistic, the methanol reactor is modeled with a restricted equilibrium approach, where the chemical equilibrium is reached in the reactor at a temperature that is 70°C above the reaction temperature. There are two hot streams (Cooler 1 and 2) and three cold streams (Heater 1, 2 and 3) in the heat integration problem. Intermediate-pressure (IP) steam (230°C) and low-pressure (LP) steam (164°C) are used as hot utilities and cooling water (20°C) is used as the cold utility. Steam can be generated in the methanol reactor because the methanol synthesis reaction is exothermic. The pressure level of the produced steam depends on the reactor temperature, that is, LP steam is produced if the reactor temperature is between 169°C and 235°C and IP steam is generated if the reactor temperature is above 235°C, assuming HRAT is 5K.

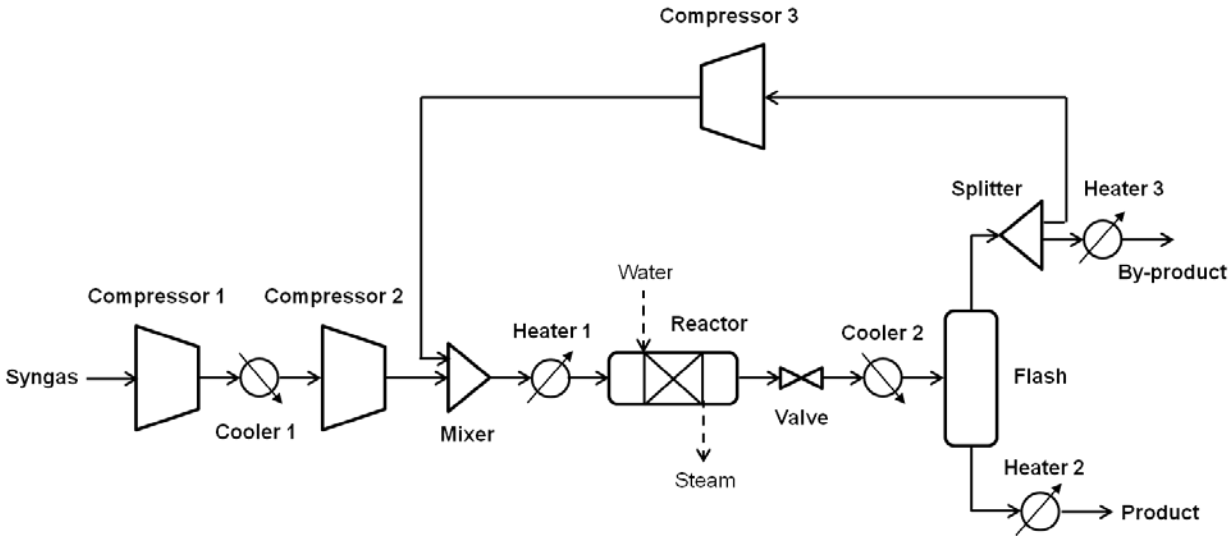

Figure 3: Process flowsheet for a methanol production process

Table 1. Information for the feedstock stream in Case 1

Description	Value	Unit
Total molar flowrate	100.0	kmol/hr
Mole fraction		
H_2	0.65	
CO	0.3	
CH_4	0.05	
Temperature	25.0	°C
Pressure	10.0	bar

Table 2. Specifications for product and by-product streams in Case 1

Specification	Value	Unit
Product Stream		
Mole fraction of CH_3OH	≥ 0.95	
Temperature	125.0	°C
Pressure	≥ 2.5	bar
By-product Stream		
Temperature	125.0	°C
Pressure	≥ 2.5	bar

The optimization model for Case 1 is formulated as in Eq.(3):

Maximize Profit (3)

s.t. Purity of methanol in the product ≥ 95.0 %

Flowsheet evaluations (via process simulators)

Minimum utility and heat exchanger area target (via heat integration module)

where the profit is calculated as: Profit = Revenue (product, by-product and steam generation) - Feedstock cost - Operational cost (hot and cold utility, electricity), and the purity of methanol is the mole fraction of methanol in the product stream. There are five decision variables to be optimized, as shown in Table 3.

Table 3. Decision variables in Case 1

Decision Variable	Lower Bound	Upper Bound
Split fraction to by-product in Splitter	0.01	0.90
Temperature of Reactor (°C)	200.0	250.0
Pressure of Reactor (bar)	25.0	50.0
Temperature of Flash (°C)	25.0	150.0
Pressure of Flash (bar)	2.5	50.0

4.1.2. Results of Optimization and Heat Integration

The simultaneous optimization and heat integration was performed for the methanol production process. The heat integration problem is formulated in GAMS 24.1 (McCarl et al., 2013), and LP models (1) and (2) are solved in CPLEX 12.0 (CPLEX, 2013). The parameter settings for the heat integration problem are listed in Table 4, which are the same in Case 1, 2 and 3. As indicated before, the process is modeled within Aspen Plus. Other price information used for the profit calculation in Case 1 is shown in Table 5.

Table 4. Parameter settings for the heat integration problem

Parameter	Value	Unit
Heat recovery approach temperature (HRAT)	5	K
Exchanger minimum approach temperature (EMAT)	2	K
Unit cost of intermediate-pressure (IP) steam (c_m)	0.804	¢/MJ
Unit cost of low-pressure (LP) steam (c_m)	0.625	¢/MJ
Unit cost of cooling water (c_n)	0.021	¢/MJ
Correction factor for non-countercurrent flow pattern (Ft)	0.81	
Film heat transfer coefficients for hot process stream (h_i)	0.8	kW/m^2/K
Film heat transfer coefficients for cold process stream (h_j)	0.8	kW/m^2/K
Film heat transfer coefficients for hot utility (h_i)	6.0	kW/m^2/K
Film heat transfer coefficients for cold utility (h_j)	3.75	kW/m^2/K

Table 5. Other price information in Case 1

Price	Value	Unit
Feedstock	2.4	$/kmol
Product	13.0	$/kmol
By-product	1.8	$/kmol
Electricity	7.0	¢/kWh

The results of three cases are compared in this study: optimized base case (without heat integration), sequential optimization and heat integration, and simultaneous optimization and heat integration. In the optimized base case without heat integration all heating and cooling loads in the process are satisfied by utilities. The hot and cold utility consumptions are calculated by summing all heating and cooling loads, and the heat integration module is disabled. In the sequential approach, heat integration is performed after

the process is optimized and is only solved once for the optimized base case. In the simultaneous approach, heat integration is performed within the optimization procedure and is solved multiple times depending on the number of iterations. The optimal values of decision variables are shown in Table 6, and the optimization and heat integration results are shown in Table 7. It is noted that we have assumed constant FCps for all process streams in the heat integration problems here. The study that considers variable FCps by using piecewise linear approximation of composite curves will be discussed later.

Table 6. Optimal values of decision variables in Case 1

Decision Variable	Optimized base case w/o heat integration (and sequential approach)	Simultaneous approach [a]
Split fraction to by-product in Splitter	0.038	0.01
Temperature of Reactor (°C)	200.0	200.0
Pressure of Reactor (bar)	50.0	50.0
Temperature of Flash (°C)	32.6	25.5
Pressure of Flash (bar)	50.0	50.0

[a] Constant FCps are assumed for all streams in the heat integration problem.

Table 7. Optimization and heat integration results in Case 1

	Optimized base case w/o heat integration	Sequential approach [a]	Simultaneous approach [a]
Profit ($/d)	3442.7	3924.8	4158.4
Revenue ($/d)	9990.1	9990.1	10249.6
Feedstock cost ($/d)	5760.0	5760.0	5760.0
Operational cost ($/d)	787.5	305.3	331.2
Methanol purity in the product (%)	98.6	98.6	98.4
Methanol product flowrate (kmol/hr)	28.7	28.7	29.9
By-product flowrate (kmol/hr)	14.6	14.6	11.1
Overall conversion	0.942	0.942	0.982
IP steam generation (kW_{th})	0.0	0.0	0.0
LP steam generation (kW_{th})	775.7	775.7	806.9
Electricity consumption (kW_e)	169.2	169.2	169.3
IP steam consumption (kW_{th})	619.1	21.5	57.4
LP steam consumption (kW_{th})	100.6	0.0	0.0
Cooling water consumption (kW_{th})	1034.7	336.5	382.1
Heat exchanger area (m^2)	n/a	160.1	660.7

[a] Constant FCps are assumed for all streams in the heat integration problem.

The methanol purity constraint (≥ 95%) is satisfied in all three cases. After heat integration, the profit is greatly increased ($3924.8/d vs. $3442.7/d) because utility consumptions are reduced and the operational cost is decreased. The simultaneous approach achieves a significantly higher profit than the sequential one ($4158.4/d vs. $3924.8/d). The major reason is that a higher overall conversion of CO is obtained in the simultaneous approach (0.982 vs. 0.942), which increases the production rate and revenue. Note that the operational cost in the simultaneous approach is actually a little higher than the sequential one because utility consumptions are increased under a higher recycle ratio (and heat exchanger area is also increased). The results demonstrate one of the major advantages of the simultaneous approach compared to the sequential approach, that is, higher conversion and product revenue, in the optimal design of chemical processes with recycles.

4.2. Case 2: Separation Process for Benzene Products

4.2.1. Process Overview

Figure 4 shows the flowsheet of a separation process for benzene products (Biegler, 2014). In this process, a feedstock containing hydrogen chloride (HCl), benzene (C_6H_6), and monochlorobenzene (MCB, C_6H_5Cl) is separated and pure benzene and MCB products are obtained. The information for the feedstock stream is shown in Table 8. The feed stream is heated and sent to a flash, after which the gas stream is sent to an HCl separation column to produce the HCl by-product and the liquid stream is mixed with the bottom stream from the HCl column. Next, the mixed stream passes through an HCl stripper to remove the remaining HCl, before being sent to the distillation column. The C_6H_6 product is extracted from the top of the column. The bottom stream from the column is cooled and passes through a splitter, where the majority of the stream is removed from the process as the C_6H_5Cl product with the remainder recycled back to the HCl column via a pump. This separation process is modeled in Aspen Plus. There are two hot

streams (cooler and condenser) and two cold streams (heater and reboiler) in the heat integration problem. LP steam (164°C) is used as the hot utility and cooling water (20°C) is used as the cold utility.

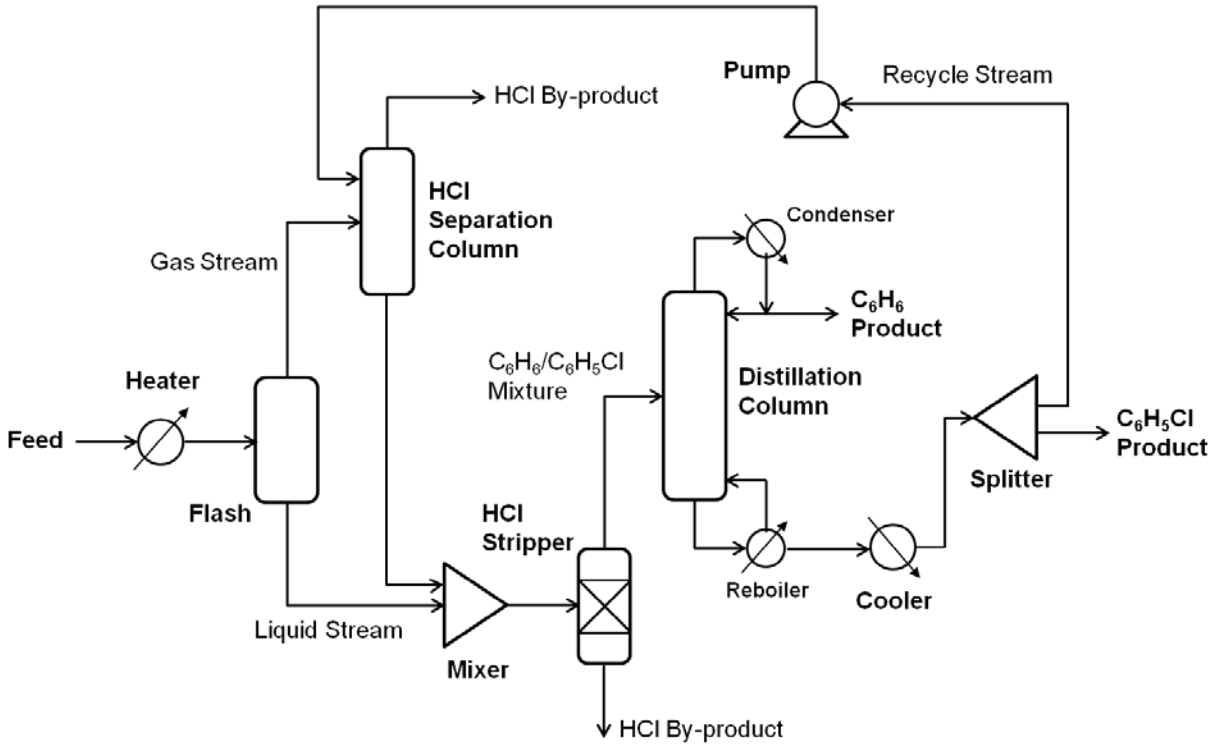

Figure 4. Process flowsheet for a benzene products separation process

Table 8. Information for the feedstock stream in Case 2

Description	Value	Unit
Total molar flowrate	45.36	kmol/hr
Mole fraction		
HCl	0.1	
C_6H_6	0.4	
C_6H_5Cl	0.5	
Temperature	26.67	°C
Pressure	2.55	bar

The optimization model for Case 2 is formulated as in Eq.(4):

Minimize Total operational cost (4)

s.t. Purity of C_6H_6 and C_6H_5Cl in the products $\geq$ 99.5 %

Recovery of C_6H_6 and C_6H_5Cl $\geq$ 99.0 %

Flowsheet evaluations (via process simulators)

Minimum utility and heat exchanger area target (via heat integration module)

where the total operational cost is the sum of utility cost (steam and cooling water) and electricity cost, the purity of C_6H_6 or C_6H_5Cl is the mole fraction of C_6H_6 or C_6H_5Cl in its product stream, and the recovery of C_6H_6 or C_6H_5Cl is the fraction of the molar flowrate of C_6H_6 or C_6H_5Cl in its product stream to that in the feedstock stream. Six decision variables are optimized, as shown in Table 9.

Table 9. Decision variables in Case 2

Decision Variable	Lower Bound	Upper Bound
Split fraction to C_6H_5Cl stream in Splitter	0.1	0.9
Distillate to feed ratio in Distillation Colum	0.1	0.9
Reflux ratio in Distillation Column	1	10
Outlet temperature of Heater (°C)	60	145
Outlet temperature of Cooler (°C)	30	50
Outlet pressure of Pump (bar)	2.2	3.5

4.2.2. Results of Optimization and Heat Integration

Results of the optimized base case (without heat integration), the sequential approach and the simultaneous approach are compared in this study. The optimal values of decision variables are shown in Table 10, and the optimization and heat integration results are shown in Table 11. Again, we assume constant FCps for all process streams in the heat integration problems.

Table 10. Optimal values of decision variables in Case 2

Decision Variable	Optimized base case w/o heat integration (and sequential approach)	Simultaneous approach [a]
Split fraction to C_6H_5Cl stream in Splitter	0.9	0.7675
Distillate to feed ratio in Distillation Colum	0.4193	0.3811
Reflux ratio in Distillation Column	1.38	1.595
Outlet temperature of Heater (°C)	60.0	90.87
Outlet temperature of Cooler (°C)	30.0	30.0
Outlet pressure of Pump (bar)	2.2	2.2

[a] Constant FCps are assumed for all streams in the heat integration problem.

Table 11. Optimization and heat integration results in Case 2

	Optimized base case w/o heat integration	Sequential approach [a]	Simultaneous approach [a]
Total operational cost ($/d)	266.9	236.3	231.3
C_6H_6 purity in the product (%)	99.50	99.50	99.50
C_6H_5Cl purity in the product (%)	99.50	99.50	99.50
C_6H_6 recovery (%)	99.27	99.27	99.29
C_6H_5Cl recovery (%)	99.00	99.00	99.00
C_6H_6 product flowrate (kmol/hr)	18.10	18.10	18.11
C_6H_5Cl product flowrate (kmol/hr)	22.57	22.57	22.57
Electricity consumption (kW_e)	0.015	0.015	0.041
LP steam consumption (kW_{th})	560.3	496.4	485.8
Cooling water consumption (kW_{th})	502.7	438.7	426.8
Heat exchanger area (m^2)	n/a	117.5	120.5

[a] Constant FCps are assumed for all streams in the heat integration problem.

Purity and recovery requirements for benzene and MCB are satisfied in all three cases. After heat integration, the operational cost is reduced ($236.3/d vs. $266.9/d) because part of heating and cooling loads in the process can be satisfied by internal heat integration instead of using utilities. Compared to the sequential approach, the simultaneous approach achieves better heat integration within the process, that is, less steam and cooling water are consumed while satisfying the same purity and recovery constraints. The optimal operating conditions have also been adjusted to implement the more efficient heat integration strategy, as shown in Table 10. Therefore, a lower operational cost is obtained ($231.3/d and $236.3/d).

4.2.3. Heat Integration with Piecewise Linear Approximation of Composite Curves

The aforementioned heat integration studies are still based on the assumption of constant FCps for all streams. However, as described previously, this assumption may overestimate the total heat recovery in the process, which means that the real objective value may not be as "good" as that predicted by the heat integration model. In this study, two heat integration methods are compared: constant FCps and a piecewise linear approximation. In the piecewise linear approximation approach, the temperature range of all streams is divided into five sub-regions, which have the same size (or range). The piecewise linear approximation is expected to obtain much more accurate heat integration results. The simultaneous optimization and heat integration is utilized in this study. The optimal values of decision variables by using the two heat integration approaches are compared in Table 12, and the optimization and heat integration results are compared in Table 13.

Table 12. Comparison of optimal values of decision variables for two heat integration methods in Case 2

Decision Variable	Constant FCps [a]	Piecewise linear approximation [a]
Split fraction to C_6H_5Cl stream in Splitter	0.7675	0.7778
Distillate to feed ratio in Distillation Colum	0.3811	0.3843
Reflux ratio in Distillation Column	1.595	1.577
Outlet temperature of Heater (°C)	90.87	88.89
Outlet temperature of Cooler (°C)	30.0	30.0
Outlet pressure of Pump (bar)	2.2	2.2

[a] Simultaneous optimization and heat integration approach is applied.

Table 13. Comparison of optimization and heat integration results for two heat integration methods in Case 2

	Constant FCps [a]	Piecewise linear approximation [a]
Total operational cost ($/d)	231.3	231.3
C_6H_6 purity in the product (%)	99.50	99.50
C_6H_5Cl purity in the product (%)	99.50	99.50
C_6H_6 recovery (%)	99.29	99.29
C_6H_5Cl recovery (%)	99.00	99.00
C_6H_6 product flowrate (kmol/hr)	18.11	18.11
C_6H_5Cl product flowrate (kmol/hr)	22.57	22.57
Electricity consumption (kW_e)	0.041	0.038
LP steam consumption (kW_{th})	485.8	485.9
Cooling water consumption (kW_{th})	426.8	426.9
Heat exchanger area (m^2)	120.5	120.1

[a] Simultaneous optimization and heat integration approach is applied.

The results of two heat integration methods are very close to each other in this case as seen in Table 13. The reason is that no stream in Case 2 shows significant variations in FCp. In particular, no stream undergoes phase change. Therefore, the assumption of constant FCps is largely valid for Case 2. This observation indicates that constant FCps hold for most of streams without phase change. It seems that piecewise linear approximation does not show any advantages in regular cases such as Case 2; however, it could be very effective in solving cases including streams with phase change, as will be discussed in Case 3.

4.3. Case 3: Supercritical Coal Power Plant with Carbon Capture and Compression

4.3.1. Process Overview

Figure 5 shows the process flowsheet for a 650 MW_{net} (before capture) supercritical pulverized coal power plant with a post-combustion solid sorbent carbon capture and compression system. Four subsystems are included in the process: the boiler, steam cycle, carbon capture system and compression system. Flue gas from the boiler passes through the capture system to remove carbon dioxide (CO_2). The captured CO_2 is desorbed and then compressed for geologic storage. The carbon capture system is

comprised of a three-stage bubbling fluidized bed (BFB) adsorber and a two-stage BFB regenerator, in which amine-impregnated mesoporous silica materials are utilized as the solid sorbent. The compression system contains multi-stage compressors with intermediate coolers. Both the carbon capture system and compression system are modeled in ACM (Miller et al., 2013). The steam cycle includes a series of turbines operated at different pressure levels and multiple feed water heaters and was developed in SteamPro and Thermoflex (Thermoflow, 2013).

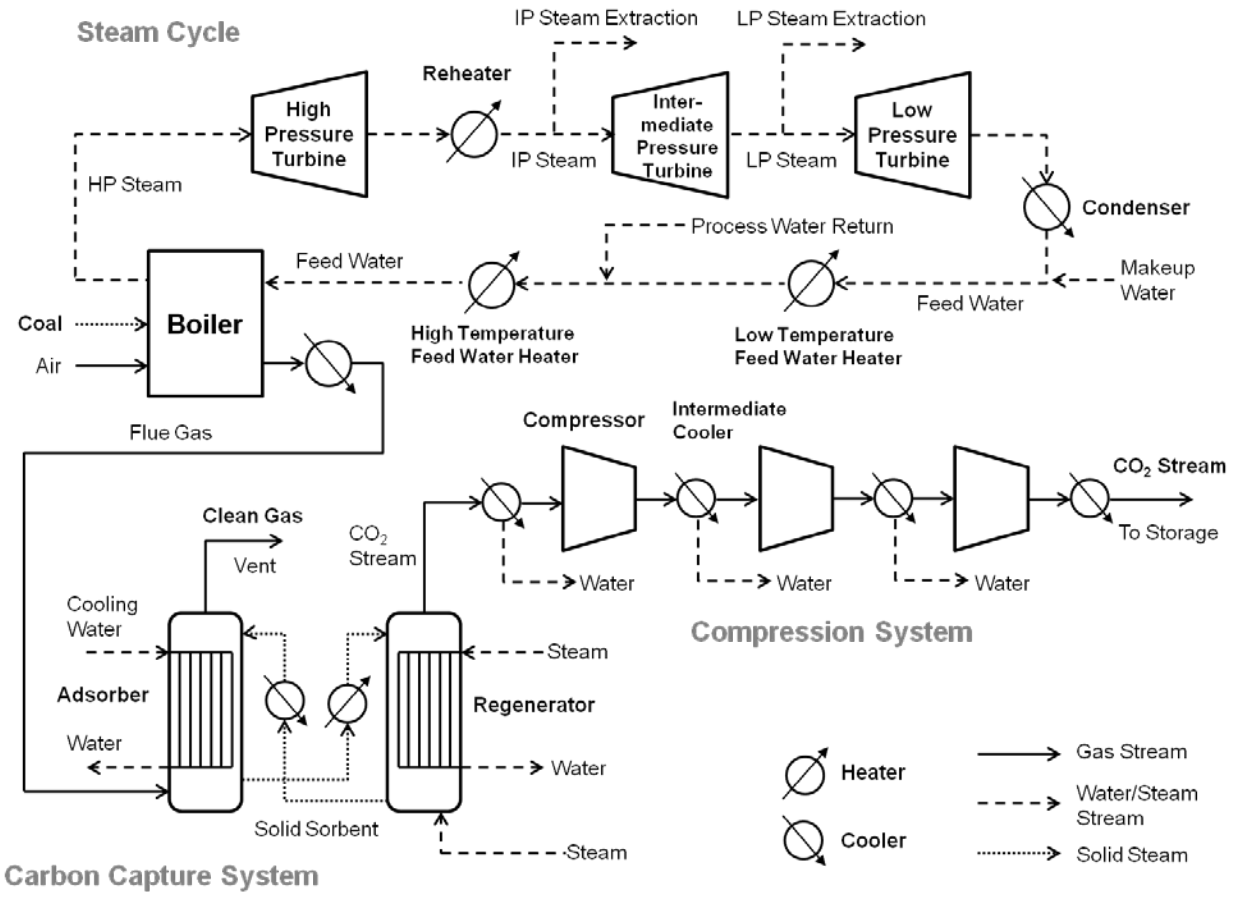

Figure 5. Process flowsheet for a supercritical pulverized coal power plant with a post-combustion, solid sorbent carbon capture and compression system

A number of heat integration opportunities are present in this process. As shown in Figure 5, boiler feed water needs to be preheated; heat needs to be removed from the adsorber and added to the regenerator in the capture system; and the CO_2 stream needs to be cooled between compressors. In total, 18 hot and 11 cold process streams are included in the heat integration subproblem. Note that in power plants, steam is usually obtained from the steam cycle instead of being purchased as an external utility. Hence, heat integration for power plants not only reduces the operational cost but also increases the net power efficiency. In this case, intermediate-pressure (IP) steam (230°C) and low-pressure (LP) steam (164°C) are extracted between the corresponding turbines. Excess heat from the capture and compression system can be recovered for use in steam cycle via the boiler feed water heaters. Correlations for net power output are derived from rigorous simulations of power plants in Thermoflex (Eslick and Chen, 2013), and are employed in this case study for calculating net efficiency of the power plant.

The optimization model for Case 3 is formulated as in Eq.(5):

Maximize Net power efficiency (5)

s.t. CO_2 removal ratio $\geq$ 90 %

Flowsheet evaluations (via process simulators)

Minimum utility and heat exchanger area target (via heat integration module)

23 decision variables are optimized, including bed lengths and diameters of adsorbers and regenerators, sorbent flow rates, steam feed rates, and outlet temperature of intermediate coolers in the compression train. The key decision variables are shown in Table 14.

Table 14. Key decision variables in Case 3

Decision Variable	Lower Bound	Upper Bound
Bed diameter of adsorbers (m)	9	15
Bed diameter of regenerators (m)	9	12
Bed length of 1st-stage adsorber (m)	2.8	4.2
Bed length of 2nd-stage adsorber (m)	2.8	4.2
Bed length of 3rd-stage adsorber (m)	2.8	4.2
Bed length of 1st-stage regenerator (m)	2.8	4.2
Bed length of 2nd-stage regenerator (m)	2.8	4.2
Solid sorbent inlet flowrate in adsorber (t/hr)	400	900
IP steam injection rate in regenerator (kmol/hr)	500	1000
Outlet temperature of CO_2 cooler before compression (°C)	30	70
Outlet temperature of 1st intercooler in compression system (°C)	30	70
Outlet temperature of 2nd intercooler in compression system (°C)	30	70
Outlet temperature of 3rd intercooler in compression system (°C)	30	70
Outlet temperature of 4th intercooler in compression system (°C)	30	70
Outlet temperature of 5th intercooler in compression system (°C)	30	70

4.3.2. Results of Optimization and Heat Integration

The net efficiency of this power plant without carbon capture and compression is 42.1%. After incorporating an optimized carbon capture and compression system without considering heat integration, the net efficiency decreases to 31.0 % due to steam extraction in the steam cycle and power consumption in the compression system. Some limited crossflow heat exchangers are typically utilized in the capture system, which however are not considered in the optimized base case here. Results of the optimized base case (without heat integration), the sequential approach and the simultaneous approach are compared in this study. Optimal values of key decision variables are listed in Table 15, and optimization and heat integration results are compared in Table 16. We assume constant FCps for all streams in heat integration problems solved here.

Table 15. Optimal values of key decision variables in Case 3

Decision Variable	Optimized base case w/o heat integration (and sequential approach)	Simultaneous approach [a]
Bed diameter of adsorbers (m)	9.61	11.92
Bed diameter of regenerators (m)	12.0	10.94
Bed length of 1st-stage adsorber (m)	2.80	3.73
Bed length of 2nd-stage adsorber (m)	2.80	4.02
Bed length of 3rd-stage adsorber (m)	2.80	2.83
Bed length of 1st-stage regenerator (m)	4.20	3.22
Bed length of 2nd-stage regenerator (m)	4.12	3.44
Solid sorbent inlet flowrate in adsorber (t/hr)	900.0	886.7
IP steam injection rate in regenerator (kmol/hr)	500.6	500.7
Outlet temperature of CO_2 cooler before compression (°C)	33.1	59.4
Outlet temperature of 1st intercooler in compression system (°C)	30.4	68.1
Outlet temperature of 2nd intercooler in compression system (°C)	30.0	47.2
Outlet temperature of 3rd intercooler in compression system (°C)	40.8	53.1
Outlet temperature of 4th intercooler in compression system (°C)	30.3	38.1
Outlet temperature of 5th intercooler in compression system (°C)	31.4	31.0

[a] Constant FCps are assumed for all streams in the heat integration problem.

Table 16. Optimization and heat integration results in Case 3

	Optimization w/o heat integration	Sequential approach [a]	Simultaneous approach [a]
Net power efficiency (%)	31.0	32.7	35.7
Net power output (MW_e)	479.7	505.4	552.4
CO_2 removal ratio (%)	90.0	90.0	90.0
Electricity consumption [b] (MW_e)	67.0	67.0	80.4
IP steam withdrawn from power cycle (MW_{th})	0	0	0
LP steam withdrawn from power cycle (MW_{th})	336.3	304.5	138.3
Cooling water consumption [b] (MW_{th})	886.8	429.3	445.1
Heat addition to feed water (MW_{th})	0	125.3	164.9
Heat exchanger area (m^2)	n/a	2.69×10^5	2.32×10^5

[a] Constant FCps are assumed for all streams in the heat integration problem.

[b] Only electricity and cooling water consumptions in capture and compression systems are included.

The target CO_2 removal ratio (90%) is satisfied in all cases. Among the most significant contributors to the ultimate cost of a carbon capture and compression system is the reduction of net power from the power plant. This is also reflected in the net power efficiency. The net efficiency is significantly increased

by performing heat integration (32.7 % vs. 31.0 %) because steam usage is reduced and more heat is recovered in steam cycle. Simultaneous optimization and heat integration achieves an even higher net efficiency (35.7 % vs. 32.7 %) and higher net power (552.4 MW_e vs. 505.4 MW_e) than the sequential approach. By applying the simultaneous approach, more heat can be recovered within the process and a smaller heat exchanger area is obtained.

4.3.3. Heat Integration with Piecewise Linear Approximation of Composite Curves

In Case 3, a number of process streams undergo phase change, especially streams containing both CO_2 and H_2O (as shown in Figure 2). The variation of FCp with temperature must be considered here to ensure accurate heat integration results. Heat integration with constant FCps and variable FCps (modeled by piecewise linear approximation) are compared as shown in Tables 17 and 18. In the piecewise linear approximation approach, the temperature range of all process streams is divided into five sub-regions with identical size.

Table 17. Comparison of optimal values of decision variables for two heat integration methods in Case 3

Decision Variable	Constant FCps [a]	Piecewise linear approximation [a]
Bed diameter of adsorbers (m)	11.92	9.16
Bed diameter of regenerators (m)	10.94	12.00
Bed length of 1st-stage adsorber (m)	3.73	2.81
Bed length of 2nd-stage adsorber (m)	4.02	2.80
Bed length of 3rd-stage adsorber (m)	2.83	2.80
Bed length of 1st-stage regenerator (m)	3.22	4.20
Bed length of 2nd-stage regenerator (m)	3.44	4.06
Solid sorbent inlet flowrate in adsorber (t/hr)	886.7	896.7
IP steam injection rate in regenerator (kmol/hr)	500.7	500.0
Outlet temperature of CO_2 cooler before compression (°C)	59.4	51.3
Outlet temperature of 1st intercooler in compression system (°C)	68.1	31.8
Outlet temperature of 2nd intercooler in compression system (°C)	47.2	49.3
Outlet temperature of 3rd intercooler in compression system (°C)	53.1	44.7
Outlet temperature of 4th intercooler in compression system (°C)	38.1	30.3
Outlet temperature of 5th intercooler in compression system (°C)	31.0	31.2

[a] Simultaneous optimization and heat integration approach is applied.

Table 18. Comparison of optimization and heat integration results for two heat integration methods in Case 3

	Constant FCps [a]	Piecewise linear approximation [a]
Net power efficiency (%)	35.7	32.1
Net power output (MW_e)	552.4	496.7
CO_2 removal ratio (%)	90.0	90.0
Electricity consumption [b] (MW_e)	80.4	69.1
IP steam withdrawn from power cycle (MW_{th})	0	0
LP steam withdrawn from power cycle (MW_{th})	138.3	303.3
Cooling water consumption [b] (MW_{th})	445.1	465.8
Heat addition to feed water (MW_{th})	164.9	90.2
Heat exchanger area (m^2)	2.32×10^5	2.54×10^5

[a] Simultaneous optimization and heat integration approach is applied.

[b] Only electricity and cooling water consumptions in capture and compression systems are included.

By using the piecewise linear approximation of the composite curve, it is found that in the original heat integration model with constant FCps the steam consumption is underestimated and heat recovery to steam cycle is overestimated. Therefore, the net efficiency after considering variable FCps is somewhat decreased (32.1% vs. 35.7%). However, this new heat integration result is much more accurate and realistic. Nonetheless, the net efficiency with heat integration is still much higher than that without (32.1 % vs. 31.0 %). This result demonstrates that the assumption of constant FCps is no longer valid for streams with phase change, and piecewise linear approximation of the composite curve is necessary to obtain accurate estimations for heat recovery.

5. Conclusions

This paper has described a novel simultaneous optimization and heat integration approach that can directly utilize rigorous simulation models within commercial process simulators. In this approach a heat integration module has been developed based on LP formulations that utilize stream information from process simulation results, and calculates the minimum utility and heat exchanger area target within the

overall optimization algorithm. This approach is relatively easy to implement and has been incorporated into FOQUS.

The simultaneous approach has been studied for a methanol production process (with recycle), a benzene products separation process and a power plant with carbon capture and compression. Compared to the sequential approach, the simultaneous approach achieves a significantly higher profit in the recycle process, a lower operational cost in the separation process and higher net power efficiency in the power plant.

The piecewise linear approximation for the composite curve is implemented in the heat integration problem to replace the assumption of constant FCps for all streams. The new heat integration approach achieves more accurate results for cases including streams with phase change or highly non-ideal thermodynamic behaviour.

Acknowledgment

The authors thank Joshua Boverhof at LBNL and Jim Leek at LLNL for their development of Turbine and SimSinter, which are critical components supporting FOQUS and the simultaneous approach. The authors also acknowledge financial support through U.S. Department of Energy, Office of Fossil Energy, National Energy Technology Laboratory (NETL) (Grant Number: 4000.2.673.062.001.641.000.004). This project was conducted as a part of the Carbon Capture Simulation Initiative (CCSI) program.

References

AspenTech. Introduction of Aspen Plus and other Aspen products. 2014. http://www.aspentech.com/products/aspen-plus/.

Baliban RC, Elia JA, Floudas CA. Optimization framework for the simultaneous process synthesis, heat and power integration of a thermochemical hybrid biomass, coal, and natural gas facility. Comput. Chem. Eng., 2011; 35:1647-1690.

Baliban RC, Elia JA, Floudas CA. Simultaneous process synthesis, heat, power, and water integration of thermochemical hybrid biomass, coal, and natural gas facilities. Comput. Chem. Eng., 2012; 37:297-327.
Biegler LT. Nonlinear Programming: Concepts, Algorithms and Applications. Courseware, Carnegie Mellon University. 2014. http://cepac.cheme.cmu.edu/pasilectures/biegler/BieglerLecture.pdf.
Biegler LT, Grossmann IE, Westerberg AW. Chapter 18: Simultaneous optimization and heat integration. Systematic Methods of Chemical Process Design. New Jersey: Prentice Hall PTR; 1997.
Boverhof J, Leek J, Eslick JC and Agarwal D. Turbine and Sinter: Enabling management of parallel process simulations on demand. CCSI Technical Report Series. 2013. http://www.acceleratecarboncapture.org.
Cerda J, Westerberg AW. Synthesizing heat exchanger networks having restricted stream/stream matches using transportation problem formulation. Chem. Eng. Sci., 1983; 38(10):1723-1740.
Chen Y, Adams TA, Barton PI. Optimal design and operation of static energy polygeneration systems. Ind. Eng. Chem. Res., 2011; 50(9):5099-5113.
Chen Y, Adams TA, Barton PI. Optimal design and operation of flexible energy polygeneration systems. Ind. Eng. Chem. Res., 2011; 50(8):4553-4566.
Chen Y, Eslick JC, Grossmann IG, Miller DC. Simultaneous optimization and heat integration based on rigorous process simulations. Proceedings of the 8th International Conference on Foundations of Computer-Aided Process Design - FOCAPD 2014. Cle Elum, Washington. 2014.
Conn AR, Scheinberg K, Vicente LN. Introduction to derivative-free optimization. Pennsylvania: Society for Industrial and Applied Mathematics; 2009.
CPLEX. Cplex Solver Manual. 2013. http://www.gams.com/dd/docs/solvers/cplex.pdf.
Čuček L, Martín M, Grossmann IE, Kravanja Z. Energy, water and process technologies integration for the simultaneous production of ethanol and food from the entire corn plant. Comput. Chem. Eng., 2011; 35(8):1547-1557.
Deng G. Simulation-based optimization. PhD thesis, University of Wisconsin-Madison. 2007.
Duran MA, Grossmann IE. Simultaneous optimization and heat integration of chemical processes. AIChE J., 1986; 32(1):123-138.
Eslick JC, Chen Y. Reference Power Plant Model User Manual, CCSI Technical Report Series. 2013. http://www.acceleratecarboncapture.org.
Eslick JC, Miller DC. A multi-objective analysis for the retrofit of a pulverized coal power plant with a CO_2 capture and compression process. Comput. Chem. Eng., 2011; 35(8):1488-1500.
Furman KC, Sahinidis NV. A critical review and annotated bibliography for heat exchanger network synthesis in the 20th century. Ind. Eng. Chem. Res., 2002; 41(10):2335-2370.
Gebreslassie BH, Slivinsky M, Wang B, You F. Life cycle optimization for sustainable design and operations of hydrocarbon biorefinery via fast pyrolysis, hydrotreating and hydrocracking. Comput. Chem. Eng., 2013; 50:71-91.
Gosavi A. Simulation-based optimization: parametric optimization techniques and reinforcement learning. Massachusetts: Kluwer Academic Publishers; 2003.
Grossmann IE, Caballero JA, Yeomans H. Mathematical programming approaches for the synthesis of chemical process systems. Korean J. Chem. Eng., 1999; 16(4):407-426.
Grossmann IE, Yeomans H, Kravanja Z. A rigorous disjunctive optimization model for simultaneous flowsheet optimization and heat integration. Comput. Chem. Eng., 1998; 22:S157-S164.
Gundersen T, Naess L. The synthesis of cost optimal heat exchanger networks: An industrial review of the state of the art. Comput. Chem. Eng., 1988; 12(6):503-530.
Gundersen T, Grossmann IE. Improved optimization strategies for automated heat exchanger network synthesis through physical insights. Comput. Chem. Eng., 1990; 14(9):925-944.
Hansen N. The CMA evolution strategy: A comparing review. Towards an New Evolutionary Computation: Studies in Fuzziness and Soft Computing, 2006; 192:75-102.
Jezowski JM, Shethna HK, Castillo FJL. Area target for heat exchanger networks using linear programming. Ind. Eng. Chem. Res., 2003; 42(8):1723-1730.
Kamath RS, Biegler LT, Grossmann IE. Modeling multistream heat exchangers with and without phase changes for simultaneous optimization and heat integration. AIChE J., 2012; 58(1):190-204.
Kim J, Kim J, Kim J, Yoo C, Moon I. A simultaneous optimization approach for the design of wastewater and heat exchange networks based on cost estimation. J. Clean. Prod., 2009; 17(2):162-171.
Klemeš JJ, Kravanja Z. Forty years of heat integration: pinch analysis (PA) and mathematical programming (MP). Current Opinion in Chemical Engineering, 2013; 2(4):461-474.

Kolda TG, Lewis RM, Torczon V. Optimization by direct search: New perspectives on some classical and modern methods. SIAM Rev., 2003; 45(3):385-482.
Lang YD, Biegler LT, Grossmann IE. Simultaneous optimization and heat integration with process simulators. Comput. Chem. Eng., 1988; 12(4):311-327.
Linnhoff B, Hindmarsh E. The pinch design method of heat exchanger networks. Chem. Eng. Sci., 1983; 38(5):745-763.
Martín M, Grossmann IE. Simultaneous optimization and heat integration for biodiesel production from cooking oil and algae. Ind. Eng. Chem. Res., 2012; 51(23):7998-8014.
McCarl BA, Meeraus A, Eijk P, Bussieck M, Dirkse S, Steacy P, Nelissen F. McCarl GAMS User Guide (Version 24.0); 2013. http://www.gams.com/dd/docs/bigdocs/gams2002/mccarlgamsuserguide.pdf.
Mele FD, Guillén G, Espuña A, Puigjaner L. A simulation-based optimization framework for parameter optimization of supply-chain networks. Ind. Eng. Chem. Res., 2006; 45(9):3133-3148.
Miller DC, Ng B, Eslick JC, Tong C, Chen Y. Advanced computational tools for optimization and uncertainty quantification of carbon capture processes. Proceedings of the 8th International Conference on Foundations of Computer-Aided Process Design - FOCAPD 2014. Cle Elum, Washington. 2014.
Miller DC, Sahinidis NV, Cozad A, Lee A, Kim H, Morinelly J, Eslick JC, Yuan Z. Computational tools for accelerating carbon capture process development. 38th International Technical Conference on Clean Coal & Fuel Systems. Clearwater, FL. 2013.
Morar M, Agachi PS. Review: Important contributions in development and improvement of the heat integration techniques. Comput. Chem. Eng., 2010; 34(8):1171-1179.
Ng RT, Tay DH, Ng DK. Simultaneous process synthesis, heat and power integration in a sustainable integrated biorefinery. Energ. Fuel., 2012; 26(12):7316-7330.
Novak Z, Kravanja Z, Grossmann IE. Simultaneous synthesis of distillation sequences in overall process schemes using an improved MINLP approach. Comput. Chem. Eng., 1996; 20(12):1425-1440.
Papalexandri KP, Pistikopoulos EN. A decomposition–based approach for process optimization and simultaneous heat integration: Application to an industrial process. Chem. Eng. Res. Des., 1998; 76(3):273-286.
Papoulias SA, Grossmann IE. A structure optimization approach in process synthesis – II. Heat recovery networks. Comput. Chem. Eng., 1983; 7(6):707-721.
Ponce-Ortega JM, Jiménez-Gutiérrez A, Grossmann IE. Simultaneous retrofit and heat integration of chemical processes. Ind. Eng. Chem. Res., 2008; 47(15):5512-5528.
Ponce-Ortega JM, Jiménez-Gutiérrez A, Grossmann IE. Optimal synthesis of heat exchanger networks involving isothermal process streams. Comput. Chem. Eng., 2008; 32(8):1918-1942.
PSE (Process Systems Enterprise). Introduction of gPROMS ModelBuilder. 2014. http://www.psenterprise.com/modelbuilder.html.
Rajasree R, Moharir AS. Simulation based synthesis, design and optimization of pressure swing adsorption (PSA) processes. Comput. Chem. Eng., 2000; 24(11):2493-2505.
Rios LM, Sahinidis NV. Derivative-free optimization: A review of algorithms and comparison of software implementations. J. Global Optim., 2013; 56(3):1247-1293.
Thermoflow. Thermoflow introduction and tutorials. 2013. http://www.thermoflow.com/convsteamcycle_STP.html.
Türkay M, Grossmann IE. Disjunctive programming techniques for the optimization of process systems with discontinuous investment costs-multiple size regions. Ind. Eng. Chem. Res., 1996; 35(8):2611-2623.
Wan X, Pekny JF, Reklaitis GV. Simulation-based optimization with surrogate models: Application to supply chain management. Comput. Chem. Eng., 2005; 29(6):1317-1328.
Wang B, Gebreslassie BH, You F. Sustainable design and synthesis of hydrocarbon biorefinery via gasification pathway: Integrated life cycle assessment and technoeconomic analysis with multiobjective superstructure optimization. Comput. Chem. Eng., 2013; 52:55-76.
Wechsung A, Aspelund A, Gundersen T, Barton PI. Synthesis of heat exchanger networks at subambient conditions with compression and expansion of process streams. AIChE J., 2011; 57(8):2090-2108.
Yang L, Grossmann IE. Water targeting models for simultaneous flowsheet optimization. Ind. Eng. Chem. Res., 2012; 52(9):3209-3224.

commercial product, process, or service by trade name, trademark, manufacturer, or otherwise does not necessarily constitute or imply its endorsement, recommendation, or favoring by the United States Government or any agency thereof. The views and opinions of authors expressed herein do not necessarily state or reflect those of the United States Government or any agency thereof.